

# Evidence of disc reflection in the X-ray spectrum of NS LMXB 4U 1636-536

Aditya S. Mondal<sup>1\*</sup>, B. Raychaudhuri<sup>1</sup>, G. C. Dewangan<sup>2</sup>

<sup>1</sup>Department of physics, Visva-Bharati, Santiniketan, West Bengal-731235, India

<sup>2</sup>Inter-University Centre for Astronomy & Astrophysics (IUCAA), Pune, 411007 India

30 September 2020

## ABSTRACT

We present a broadband spectral analysis of the atoll source 4U 1636-536 observed for  $\sim 92$  ks with *NuSTAR*. The source was found to be in a low-luminosity state during this observation with 3–79 keV X-ray luminosity of  $L_{3-79\text{keV}} = (1.03 \pm 0.01) \times 10^{37}$  ergs/s, assuming a distance of 6 kpc. We have identified and removed twelve type-I X-ray bursts during this observation to study the persistent emission. The continuum is well described by a thermal Comptonization model *nthcomp* with  $\Gamma \sim 1.9$ ,  $kT_e \sim 28$  keV, and  $kT_s \sim 0.9$  keV. The *NuSTAR* data reveal a clear signature of disc reflection, a significantly broad Fe-K emission line (around 5–8 keV), and the corresponding reflection hump (around 15–30 keV). By modelling the spectrum with a self-consistent relativistically blurred reflection model, we find that the inner disc is truncated with an inner radius of  $R_{in} = (3.2 - 4.7) R_{ISCO} (\simeq 16 - 24 R_g \text{ or } 36 - 54 \text{ km})$ . This inner disc radius suggests that the neutron star magnetic field strength is  $B \leq 2.0 \times 10^9$  G.

**Key words:** accretion, accretion discs - stars: neutron - X-rays: binaries - stars: individual 4U 1636-536

## 1 INTRODUCTION

A neutron star low mass X-ray binary system (NS LMXB) consists of a neutron star (NS) and a low mass ( $\leq 1 M_\odot$ ) companion star. When the NS in an NS LMXB accretes matter from the companion star via Roche-lobe overflow, a geometrically thin, optically thick disc-like structure is formed (Shakura & Sunyaev 1973). The radiation spectrum from the accretion disc, which is usually accompanied by a hot corona is quasi-thermal in nature and is well known to be multicolor blackbody. The inverse Compton scattering of the thermal disc photon generates a power-law spectrum. Moreover, a hot single-temperature blackbody emission may arise from the boundary layer between the inner accretion disc and the NS surface. Hard X-rays (either a power-law continuum or a blackbody component) can illuminate the accretion disc and produce a reflection spectrum which consists of several emission lines and a broad hump-like shape.

The fluorescent Fe K $\alpha$  line is the most prominent emission line due to its large cosmic abundance and high fluorescent yield (Bhattacharyya & Strohmayer 2007; Cackett et al. 2008; Pandel et al. 2008; Reis et al. 2009; Degenaar et al. 2015). In the reflection spectrum, a broad

hump-like shape is seen which is created by the high energy photons which tend to Compton scatter back out of the disc (Ballantyne et al. 2001; Ross & Fabian 2007). Although the Fe K $\alpha$  line is intrinsically narrow as expected, it becomes broad and asymmetric in the X-ray spectrum of the LMXBs due to the Doppler and the Gravitational shift (Fabian et al. 2000). A profound study of this line profile is important due to its ability to provide information on the inner accretion flow in the NS LMXBs which in turn provides constraints to the structure of the inner disc and inclination. In an NS binary system, the accretion disc may be truncated by a strong stellar magnetic field or by the boundary layer between the disc and the NS outer surface. The upper limit to the radius of the NS is related to the inner disc radius and may constrain the NS EOS (Piraino et al. 2000; Cackett et al. 2008; Bhattacharyya 2011). Moreover, the Fe K $\alpha$  line is also used to find out an upper limit to the strength of the magnetic field related to the NS (Ludlam et al. 2019; Degenaar et al. 2016; King et al. 2016).

4U 1636-536 is an atoll type, bursting LMXB consisting of an NS and an 18th magnitude,  $0.4 M_\odot$  companion star (van Paradijs et al. 1990). The source has been studied extensively in the literature. The source has exhibited type-I X-ray bursts, double-peaked X-ray bursts, superbursts, Quasi-Periodic Oscillations (QPOs), and millisecond oscil-

\* E-mail: adityas.mondal@visva-bharati.ac.in

lation during thermonuclear bursts (Wijnands et al. 1997; Galloway et al. 2006; Strohmayer & Markwardt 2002). It has an orbital period of  $\sim 3.8$  hr (van Paradijs et al. 1990). Its location has been estimated to be  $6 \pm 0.5$  kpc by Galloway et al. (2006) who also studied its type-I X-ray bursts. This source is known to show QPOs (Wijnands et al. 1997; Zhang et al. 1996; Barret et al. 2007) at the domain of kHz. The inclination has been suggested to lie in the range  $\sim 30 - 60^\circ$  from optical observations (Casares et al. 2006). The source is well known to show burst oscillations at 581 Hz which is remarkably coherent (Strohmayer & Markwardt 2002). This is possibly related to the rotation of the NS. The soft X-ray emission, modulated at the QPO frequency of kHz range is known to have a phase lag behind the hard X-ray emission (Kaaret et al. 1999). This lag could be produced by the reprocessing of hard X-rays in a cooler Comptonizing corona with a size of at most a few kilometers.

Pandel et al. (2008) analysed the *XMM-Newton* and *RXTE* data of the source 4U 1636-536. They found clear evidence of a broad, asymmetric iron emission line extending over the energy range 4 – 9 keV. They reported that the line profile is consistent with relativistically broadened Fe K $\alpha$  emission line from the accretion disc. They found a high disc inclination of  $36^\circ - 74^\circ$ . They reported an upper limit of the inner disc radius ( $R_{in}$ ) which is larger than the ISCO. Agrawal & Hasan (2016) analysed four simultaneous *NuSTAR* and *SWIFT* observations of the source 4U 1636-536 in the 1 – 79 keV energy band. They also observed a broad iron emission line. During these observations, the source flux varied from  $1.4 \times 10^{-9}$  to  $4.36 \times 10^{-9}$  ergs s $^{-1}$  cm $^{-2}$  and the inner disc radius varied from 6.8 to 25  $GM/c^2$ .

In this work, we present a broadband *NuSTAR* observation of the source 4U 1636-536. We search for the presence of reflection features and place constraints on the position of the inner disc. In the presence of high quality, pile-up free *NuSTAR* data and with the correct astrophysical model, X-ray reflection spectroscopy can be quite a powerful tool to probe the accretion geometry. The paper is structured in the following format: Sec.2 presents the observations and the details of data reduction. Sec.3 discusses spectral analysis and results and Sec. 4 provides the discussion of the results.

## 2 OBSERVATION AND DATA REDUCTION

*NuSTAR* (Harrison et al. 2013) observed the source 4U 1636-536 on 2019 April 27 for a total exposure time of  $\sim 92$  ks (Obs. ID: 30401014002). The data were collected with the two co-aligned grazing incidence hard X-ray imaging Focal Plane Modules (FPM) A and B telescopes in the 3 – 79 keV energy band.

The data were reduced with the standard *NuSTAR* data analysis software (*NuSTARDAS* v1.7.1) and *CALDB* (v20181030). We applied the standard routine *nupipeline* (version v 0.4.6) to filter the event lists. Using the *nuproducts* tool we created lightcurve, spectra, and response files for both the telescopes FPMA and FPMB. To

produce a source spectrum for both the telescopes, we extracted a circular region with a radius of 100 arcsec centered around the source position. We extracted the background spectrum from a same-sized radial region away from the source. We grouped the FPMA and the FPMB spectral data with a minimum of 100 counts per bin and fitted the two spectra simultaneously.

## 3 SPECTRAL FITTING

The source 4U 1636-536 is known to exhibit type-I X-ray bursts. The *NuSTAR* FPMA and FPMB light curves contain 12 type-I X-ray bursts which are shown in Figure 1. We have also shown the light curve after removing the time interval when the type-I X-ray bursts occur. The source was detected at an average intensity of  $\sim 38$  counts/s during the non-burst period. After excluding all the type-I X-ray bursts, we have fitted both the *NuSTAR* FPMA and FPMB spectra simultaneously as the initial fits have showed a good agreement between these two spectra. An initial inspection of the FPMA and the FPMB spectra also suggests that the source is detected significantly in the entire energy bandpass of the *NuSTAR*. We have therefore performed the spectral analysis over the entire 3 – 79 keV energy band using *XSPEC* v 12.9 (Arnaud 1996). Due to flux variations between the detectors, we have added a multiplicative constant in each fit. We have fixed the constant for the FPMA spectrum to unity and allowed it to vary for the FPMB spectrum. A value of 1.002 has been measured for the FPMB spectrum. We have used the *tbabs* model to account for absorption along the line of sight to the source with the abundance set to *wilm* (Wilms et al. 2000) and *vern* cross sections (Verner et al. 1996). We have fixed the absorption column density to the Dickey & Lockman (1990) value of  $4.1 \times 10^{21}$  cm $^{-2}$  as the *NuSTAR* low-energy bandpass cuts off at 3 keV and have found it difficult to constrain from the spectral fits. All quoted uncertainties in this paper are at 90% of the confidence level if not stated otherwise in particular.

### 3.1 Continuum modeling

This *NuSTAR* observation has detected the source 4U 1636-536 with a luminosity of  $\sim 1.03 \times 10^{37}$  erg/s which corresponds to  $\sim 5\%$  of the Eddington luminosity ( $L_{Edd}$ ). So, the source is detected in a low-luminosity state with  $L/L_{Edd}$  in the range of 0.05 – 0.1. The spectra of the low-luminosity state sources are typically characterized by a thermal Comptonization model with an electron temperature ( $kT_e$ ) around 25 – 30 keV (Barret et al. 2000). In the low-luminosity state, a soft component may be observed probably to represent the unscattered emission from an optically thick accretion disk (Barret et al. 2000). Additionally, Lin et al. (2007) also suggested that low/hard state spectra could be modelled with a cutoff power-law component and a single-temperature blackbody component when needed.

We have modeled the continuum above 3 keV using only a thermal Comptonization model *nthcomp* (Zdziarski et al. 1996; Życki et al. 1999) which may arise from either a hot

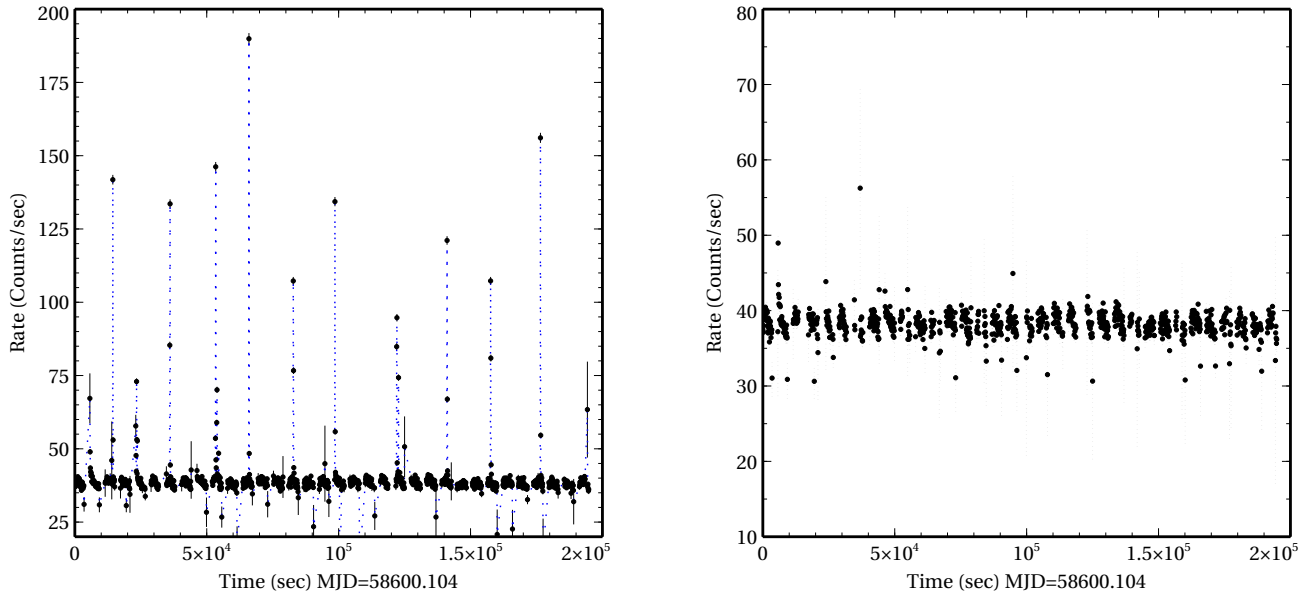


**Figure 1.** Left: 3 – 79 keV *NuSTAR*/FPMA light curve of 4U 1636-536 with a binning of 100 sec. It shows the presence of 12 brief type-I X-ray bursts. Right: Light curve after removing all the type-I X-ray bursts. In this observation, the source detected with an average intensity of  $\sim 38$  counts/s.

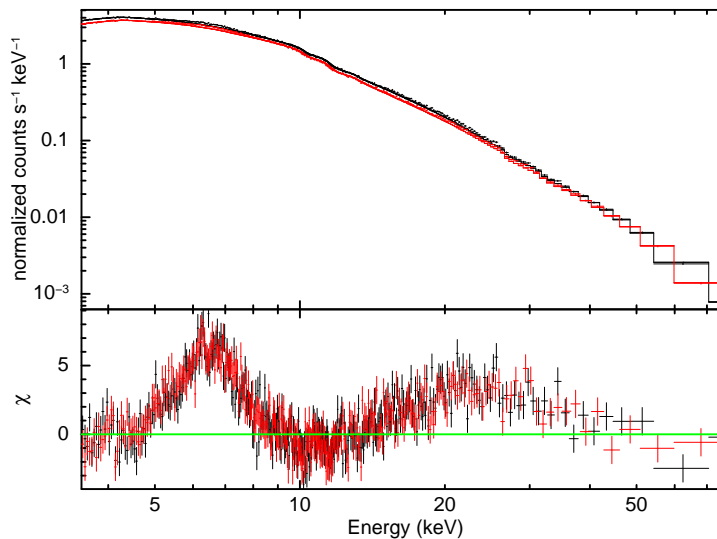


**Figure 2.** *NuSTAR* (FPMA in black, FPMB in red) unfolded spectra. The data were fit with an absorbed, thermal Comptonization model *nthcomp*. There are prominent residuals at  $\sim 5 - 8$  keV and  $\sim 10 - 20$  keV. Those can be identified as a broad Fe-K emission line and the corresponding Compton back-scattering hump. The spectral data were rebinned for visual clarity

corona associated with accretion disc or a boundary layer between the disc and the NS surface (see e.g. King et al. 2016; Ludlam et al. 2019). This thermal Comptonization model has a power-law component with an index  $\Gamma$ , a low energy cutoff determined by the temperature of the seed-photons ( $kT_s$ ) and a high energy roll-over determined by the electron temperature ( $kT_e$ ). Here we have assumed that the seed spectrum is a multi-temperature blackbody spectrum emitted from the disc. In our fits, we have allowed both these temperatures and the power-law index to vary. This model describes the continuum very well with  $\chi^2/dof = 4412/1880$ . For the *nthcomp* component, we have obtained  $\Gamma \sim 1.9$ ,  $kT_e \sim 28$  keV, and  $kT_s \sim 0.9$  keV. This continuum

model has left large positive residuals around  $\sim 5 - 8$  keV and  $\sim 15 - 30$  keV, which can be identified as a broad Fe-K emission line and the corresponding Compton hump (see Figure 2). However, it may be noted that we have not detected any soft blackbody component in the spectrum. It may possibly be due to the inadequate low-energy coverage as in the case of *NuSTAR*.

### 3.2 Reflection Modelling

As our continuum fit indicates the presence of reflection features (see Figure 2), we, therefore, have proceeded by modelling our data with a physical reflection model.

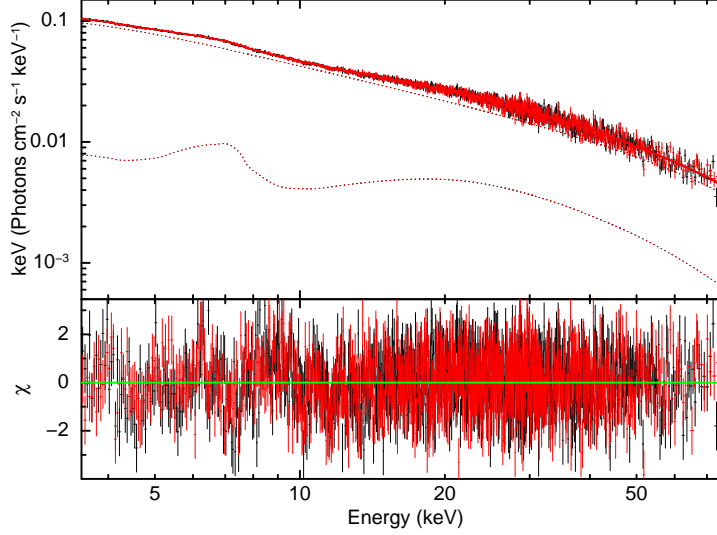


**Figure 3.** The *NuSTAR* (FPMA in black, FPMB in red) unfolded spectra of 4U 1636–536 with the best-fitting fitted model consisting of a thermal Comptonization model and a relativistically blurred reflection model i.e.,  $\text{TBabs} \times (\text{nthcomp} + \text{highecut} * \text{relconv} * \text{reflionx})$ . Lower panel shows residuals in units of  $\sigma$ .

We have applied the standard **reflionx** (Ross & Fabian 2005) model that assumes a high energy exponential cutoff power-law irradiating the accretion disc. The model components of **reflionx** model are as follows:  $\Gamma$  is the photon index of the illuminating spectrum,  $\xi$  is the disc ionization parameter,  $A_{\text{Fe}}$  is the iron abundance relative to the solar value,  $N_{\text{norm}}$  is the normalization of the reflected spectrum and  $z$  is the redshift of the source.

We have modified this reflection model **reflionx** in such a way that it assumes **nthcomp** illuminating spectrum instead of a cutoff power-law, as our broad-band fits prefer a Comptonized model to describe the continuum spectrum. The cutoff power-law does not have a low-energy cutoff while Comptonization spectra require a low-energy cutoff at the seed photon temperature ( $kT_s$ ). Moreover, the high energy cutoff of the illuminating power law in the **reflionx** model is set to 300 keV. Therefore, we have modified **reflionx** in such a manner that it mimics the **nthcomp** continuum. In order to introduce low and high energy cutoff, we have multiplied **reflionx** by a high energy cutoff, **highecut**, with the folding energy  $E_{\text{fold}}$  set to  $\sim 3$  times of the electron temperature  $kT_e$  and the cutoff energy  $E_{\text{cutoff}}$  tied to 0.1 keV. This is how we have introduced a cutoff in the reflection continuum. Moreover, we fixed the photon index ( $\Gamma$ ) of the illuminating spectrum to that of the **nthcomp** component. Thus, we have modified the reflection model **reflionx** in order to reproduce the **nthcomp** continuum by introducing the model component **highecut** (for details see Matrangola et al. 2017; Mondal et al. 2020). To take relativistic blurring into account, we have convolved **reflionx** with **relconv** component (Dauser et al. 2010). Its parameters include the inner and the outer disc emissivity indices ( $q_{\text{in}}, q_{\text{out}}$ ), break radius ( $R_{\text{break}}$ ), the inner and outer disk radii  $R_{\text{in}}$  and  $R_{\text{out}}$ , the disk inclination ( $i$ ) and the dimensionless spin parameter ( $a$ ).

We have imposed a few reasonable conditions when

making fits with reflection models. We have assumed an unbroken emissivity profile with a fixed slope of  $q = 3$ , as the slope is not constrained by the data. We have also fixed the outer disc radius  $R_{\text{out}}$  to  $1000 R_g$ . We set a redshift of  $z = 0$  since 4U 1636–536 is a Galactic source. From previous measurements of the NS spin frequency 581 Hz, we have approximated the spin parameter  $a = 0.27$  as  $a \simeq 0.47/P_{\text{ms}}$  (Braje et al. 2000) where  $P_{\text{ms}}$  is the spin period in ms. Furthermore, we have fixed the disc inclination,  $i$ , to  $60^\circ$  as it was poorly constraint when left free to vary (see also Pandel et al. 2008; Agrawal & Hasan 2016). Moreover, prior knowledge of disc inclination can significantly reduce the uncertainty of the measurement of the inner disc radius (Pandel et al. 2008).

Adding the relativistic reflection significantly improves our spectral fits with a  $\chi^2/\text{dof} = 2178/1876 = 1.16$ . The best fit parameters for the continuum and the reflection spectrum are listed in Table 1. The reflection component implies a large disc truncation prior to the ISCO at  $(3.2 - 4.7) R_{\text{ISCO}}$  ( $\simeq 16 - 24 R_g$  or  $36 - 54$  km). This model yields an intermediate disc ionization of  $\xi \sim 223$  erg  $\text{s}^{-1}$  cm which is consistent with  $\log \xi \sim (2 - 3)$  seen in other NS LMXBs (see e.g. Cackett et al. 2010). The Fe abundance obtained is consistent with solar composition ( $A_{\text{Fe}} = 1.45 \pm 0.26$ ). The fitted spectrum with relativistically blurred reflection model and the residuals are shown in the Figure 3. We have computed the distribution of  $\Delta\chi^2$  for the parameter inner disc radius ( $R_{\text{in}}$ ) using **steppar** command in **xspec** to determine how the goodness-of-fit changed as a function of this parameter. Figure 4 indicates that  $R_{\text{in}}$  is well constrained by the data. Moreover, it shows that  $R_{\text{in}}$  is inconsistent with the position of the ISCO, indicating that it is truncated far from the NS surface.

It may be noted that the reflection features are better explained by the utilization of the self-consistent reflection model RELXILL. Some new flavors of the RELXILL model are

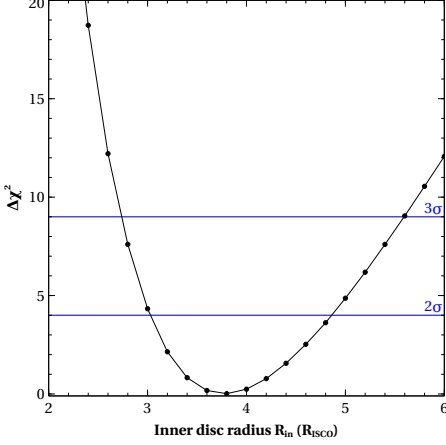


**Figure 4.** Shows the variation of  $\Delta\chi^2 (= \chi^2 - \chi^2_{min})$  as a function of inner disc radius (in the unit of  $R_{ISCO}$ ) obtained from the relativistic reflection model. We varied the inner disc radius as a free parameter in between  $2 R_{ISCO}$  to  $6 R_{ISCO}$ . The parameter is clearly well constrained by the data. The value of the inner disc radius is inconsistent with the position of the ISCO. Horizontal lines are indicating  $2\sigma$  and  $3\sigma$  significance level.

available today. A flavor of the **RELXILL** model, **RELXILLCP**, uses **nthcomp** as a illuminating continuum. This model has a hard-coded seed photon temperature of 0.05 keV. This model may not be appropriate to describe this spectral state as we detect a higher seed photon temperature of  $\sim 0.9$  keV in our continuum fit with **nthcomp**. Therefore, we did not attempt to use **RELXILLCP**.

#### 4 DISCUSSION

We have presented here a broadband spectral analysis of the *NuSTAR* observation of the source 4U 1636-536, aimed to study the reflection spectrum and to constraint the accretion geometry. The continuum spectrum is hard and well described by a thermal Comptonization model **nthcomp** with  $\Gamma \sim 1.9$ ,  $kT_e \sim 28$  keV, and  $kT_s \sim 0.9$  keV. For the first time, we have detected a clear signature of disc reflection in its spectrum. The most prominent disc reflection features, a broad Fe-K emission line around 5 – 8 keV and the corresponding Compton hump around 15 – 30 keV are clearly visible in the spectrum. A correct choice of self-consistent relativistically blurred disc reflection model helps us to determine the position of the inner disc along with some other important NS parameters. The 3 – 79 keV persistent spectrum is well described by a combination of the Comptonization model **nthcomp** and a relativistic reflection of this Comptonized emission **relconv\*reflionx**. It may be physically interpreted as the region of main energy release, where hard X-rays are produced would be either an optically thin boundary layer between the disc and the NS surface or a hot corona associated with the disc. A part of this hard X-ray emission may illuminate the accretion disc and produces the reflection spectrum.

The source was detected at an average intensity of  $\sim 38$  counts/s during the non-burst state. Our best-fit model yield an unabsorbed flux in the 3 – 79 keV band

**Table 1.** Best-fitting spectral parameters of the *NuSTAR* observation of the source 4U 1636-536 using model: **TBabs** $\times$ (**nthcomp**+**highecut**\***relconv**\***reflionx**).

Component	Parameter (unit)	Value
TBABS	$N_H (\times 10^{21} \text{ cm}^{-2})$	4.0(f)
NTHCOMP	$\Gamma$	$1.93 \pm 0.01$
	$kT_e$ (keV)	$28.8^{+3.9}_{-2.8}$
	$kT_s$ (keV)	$0.99 \pm 0.03$
	norm	$0.13 \pm 0.003$
HIGHECUT	$E_{cut}$ (keV)	0.1(f)
	$E_{fold}$ (keV)	$\simeq 3kT_e$
RELCONV	$i$ (degrees)	60(f)
	$R_{in} (\times R_{ISCO})$	$3.8^{+0.9}_{-0.6}$
REFLIONX	$\xi (\text{erg cm s}^{-1})$	$223^{+8}_{-6}$
	$\Gamma$	$1.93 \pm 0.01$
	$A_{Fe} (\times \text{solar})$	$1.45 \pm 0.25$
	norm ( $\times 10^{-5}$ )	$1.65 \pm 0.21$
	$F_{total}^* (\times 10^{-9} \text{ ergs/s/cm}^2)$	$2.4 \pm 0.01$
	$F_{nthcomp} (\times 10^{-9} \text{ ergs/s/cm}^2)$	$1.9 \pm 0.01$
	$F_{reflionx} (\times 10^{-9} \text{ ergs/s/cm}^2)$	$0.5 \pm 0.01$
	$L_{3-79\text{keV}} (\times 10^{37} \text{ ergs/s})$	$1.03 \pm 0.01$
$\chi^2/dof$		2178/1876

**Note:** Here we have used the standard **reflionx** model that assumes a high energy exponential cutoff power-law irradiating the accretion disc, modified in such a manner that it mimics the **nthcomp** continuum (see text). The outer radius of the **relconv** spectral component was fixed to  $1000 R_g$ . We fixed emissivity index  $q = 3$ . The  $E_{fold}$  parameter is fitted to be 3 times the  $kT_e$ .

\*All the unabsorbed fluxes are calculated in the energy band 3 – 79 keV

of  $F_{3-79} \sim 2.4 \times 10^{-9} \text{ ergs s}^{-1} \text{ cm}^{-2}$ , which is consistent with Agrawal & Hasan (2016). The source was observed in a low luminosity and hard spectral state (low/hard) during this observation and we measured a 3 – 79 keV luminosity of  $L_X \sim 1.03 \times 10^{37} \text{ ergs s}^{-1}$  which corresponds to  $\sim 5\%$  of the Eddington luminosity assuming a distance of 6 kpc. It suggests that the rate of any outflow in 4U 1636-536 is significantly below the Eddington mass accretion rate. It also allows us to study the disc reflection of NS LMXBs in a relatively low accretion regime.

From the reflection spectrum, we have measured a inner disc radius of  $R_{in} = (3.2 - 4.7) R_{ISCO}$ , given that



$R_{ISCO} = 5.1 GM/c^2$  for an NS spinning at  $a \simeq 0.3$ . This would correspond to  $R_{in} = (16-24) R_g$  or  $(36-54)$  km for a  $1.5 M_\odot$  NS. It indicates that the disc is truncated at a large distance away from the NS surface. The disc has a relatively low ionization ( $\xi \sim 223 \text{ erg s}^{-1} \text{ cm}$ ) and iron abundance is comparable to the solar abundance ( $A_{Fe} \sim 1.4$ ). We have detected a significantly broader Fe K $\alpha$  emission line ( $\sigma \sim 0.98 \text{ keV}$ ) from this source. The broadness of the line requires it to be located deep within the potential well where the orbital velocities are mildly relativistic (see also King et al. 2016). Moreover, the observed symmetric nature (a broad blue wing in addition to the broad red wing) of the Fe K $\alpha$  line profile requires it to be located far enough away as to not suffer severe relativistic Doppler beaming (see also King et al. 2016). Pandel et al. (2008) suggests that such a broader Fe K $\alpha$  line needs a higher disc inclination of around  $60^\circ - 70^\circ$ .

Disc truncation is likely the result of the presence of a boundary layer that lies between the disc and the NS surface or the associated magnetic field of the NS. Here we estimate the mass accretion rate ( $\dot{m}$ ) per unit area at the NS surface using Equation (2) of Galloway et al. (2008). The estimated value of  $\dot{m}$  during this observation to be  $\sim 1.6 \times 10^{-9} M_\odot \text{ y}^{-1}$  using the persistent flux  $F_p = 2.4 \times 10^{-9} \text{ erg s}^{-1} \text{ cm}^{-2}$  and assuming the bolometric correction  $c_{bol}$  is  $\sim 1.38$  for the nonpulsing sources (Galloway et al. 2008) and considering  $1 + z = 1.31$  for a NS with mass  $1.5 M_\odot$  and radius 10 km where  $z$  is the surface redshift. At this mass accretion rate, we estimate the maximum radial extent ( $R_{max}$ ) of the boundary layer region using Equation (2) of Popham & Sunyaev (2001). It estimates a maximum radial extent of  $\sim 5.4 R_g$  for the boundary layer (assuming  $M_{NS} = 1.5 M_\odot$  and  $R_{NS} = 10 \text{ km}$ ). The extent of the boundary layer region is small to account for the disc position. It may be because it does not account for a spin and viscous effects in this layer.

The inferred radial extension of the boundary layer is small compared to the disc truncation radius and the magnetic field of the NS would be responsible for the disc truncation. We can use our measured inner disc radius to estimate an upper limit for the magnetic field strength of the NS. We use Equation (1) of Cackett et al. (2009) to calculate the magnetic dipole moment ( $\mu$ ). We estimate a bolometric flux of  $F_{bol} \simeq 2.94 \times 10^{-9} \text{ erg cm}^{-2} \text{ s}^{-1}$  by extrapolating the best fit over the  $0.01 - 100 \text{ keV}$  range. We assume an NS of mass  $1.5 M_\odot$ , radius 10 km, and distance of 6 kpc. We keep similar assumptions regarding the geometrical and efficiency parameters as in Cackett et al. (2009):  $k_A = 1$  which is a factor depending on the geometry, spherical or disk-like, of the accretion flow,  $f_{ang} = 1$  which is known as the anisotropy correction factor and accretion efficiency in the Schwarzschild metric  $\eta = 0.1$ . The constraint that  $R_{in} \leq 24 R_g$  from the best fit model, then yields  $B \leq 2.0 \times 10^9 \text{ G}$  at the magnetic poles.

In this observation, we have observed 12 brief (10–100s) X-ray bursts. Accretion onto NS in LMXBs provides the fuel for thermonuclear burning that powers X-ray bursts. Therefore, the detection of X-ray bursts indicates that accreted material is still reaching the surface of 4U 1636-

536, even when the disc is truncated at a larger distance. This behavior can be explained with the model proposed by Kluzniak & Wilson (1991). They suggest that in this scenario accreted material can free-fall crossing the 'gap' between the disc and the NS surface and then strike the NS surface, creating a hot accretion belt with a temperature inversion. According to Lamb et al. (1977) the accreted material can reach the NS via a magnetic gate but it requires a relatively low magnetic field. If the accreted material is channeled along the magnetic field lines, it would cause a hot spot on the magnetic pole (Lamb et al. 2009). However, any further possible mechanisms for accretion onto the NS are out of the scope of this work. Moreover, these studies can further be extended to investigate how the accretion disc responds to an X-ray burst and the impact of bursts on the accretion disc dynamics.

## 5 DATA AVAILABILITY STATEMENT

This data set with Obs. ID: 30401014002 dated 27.04.2019 is in public domain put by NASA at their website <https://heasarc.gsfc.nasa.gov>. The public date is 08.05.2020.

## 6 ACKNOWLEDGEMENTS

This research has made use of data and/or software provided by the High Energy Astrophysics Science Archive Research Centre (HEASARC). This research also has made use of the *NuSTAR* data analysis software (NuSTARDAS) jointly developed by the ASI science center (ASDC, Italy) and the California Institute of Technology (Caltech, USA). ASM and BR would like to thank Inter-University Centre for Astronomy and Astrophysics (IUCAA) for their hospitality and facilities extended to them under their Visiting Associateship Programme.

## REFERENCES

- Agrawal V. K., Hasan M., 2016, arXiv e-prints, arXiv:1611.09004
- Arnaud K. A., 1996, in *Astronomical Society of the Pacific Conference Series*, Vol. 101, *Astronomical Data Analysis Software and Systems V*, Jacoby G. H., Barnes J., eds., p. 17
- Ballantyne D. R., Ross R. R., Fabian A. C., 2001, *MNRAS*, 327, 10
- Barret D., Olive J. F., Boirin L., Done C., Skinner G. K., Grindlay J. E., 2000, *ApJ*, 533, 329
- Barret D., Olive J.-F., Miller M. C., 2007, *MNRAS*, 376, 1139
- Bhattacharyya S., 2011, *MNRAS*, 415, 3247
- Bhattacharyya S., Strohmayer T. E., 2007, *ApJL*, 664, L103
- Braje T. M., Romani R. W., Rauch K. P., 2000, *ApJ*, 531, 447
- Cackett E. M., Altamirano D., Patruno A., Miller J. M., Reynolds M., Linares M., Wijnands R., 2009, *ApJL*, 694, L21
- Cackett E. M. et al., 2010, *ApJ*, 720, 205
- Cackett E. M. et al., 2008, *ApJ*, 674, 415

- Casares J., Cornelisse R., Steeghs D., Charles P. A., Hynes R. I., O'Brien K., Strohmayer T. E., 2006, *MNRAS*, 373, 1235
- Dauser T., Wilms J., Reynolds C. S., Brenneman L. W., 2010, *MNRAS*, 409, 1534
- Degenaar N. et al., 2016, *MNRAS*, 461, 4049
- Degenaar N., Miller J. M., Chakrabarty D., Harrison F. A., Kara E., Fabian A. C., 2015, *MNRAS*, 451, L85
- Dickey J. M., Lockman F. J., 1990, *ARAAS*, 28, 215
- Fabian A. C., Iwasawa K., Reynolds C. S., Young A. J., 2000, *PASP*, 112, 1145
- Galloway D. K., Muno M. P., Hartman J. M., Psaltis D., Chakrabarty D., 2008, *ApJS*, 179, 360
- Galloway D. K., Psaltis D., Muno M. P., Chakrabarty D., 2006, *ApJ*, 639, 1033
- Harrison F. A. et al., 2013, *ApJ*, 770, 103
- Kaaret P., Piraino S., Ford E. C., Santangelo A., 1999, *ApJl*, 514, L31
- King A. L. et al., 2016, *ApJl*, 819, L29
- Kluźniak W., Wilson J. R., 1991, *ApJl*, 372, L87
- Lamb F. K., Boutloukos S., Van Wassenhove S. o., Chamberlain R. T., Lo K. H., Clare A., Yu W., Miller M. C., 2009, *ApJ*, 706, 417
- Lamb F. K., Fabian A. C., Pringle J. E., Lamb D. Q., 1977, *ApJ*, 217, 197
- Lin D., Remillard R. A., Homan J., 2007, *ApJ*, 667, 1073
- Ludlam R. M. et al., 2019, *ApJ*, 873, 99
- Matranga M., Di Salvo T., Iaria R., Gambino A. F., Burderi L., Riggio A., Sanna A., 2017, *A&A*, 600, A24
- Mondal A. S., Dewangan G. C., Raychaudhuri B., 2020, *MNRAS*, 494, 3177
- Pandel D., Kaaret P., Corbel S., 2008, *ApJ*, 688, 1288
- Piraino S., Santangelo A., Kaaret P., 2000, *A&A*, 360, L35
- Popham R., Sunyaev R., 2001, *ApJ*, 547, 355
- Reis R. C., Fabian A. C., Young A. J., 2009, *MNRAS*, 399, L1
- Ross R. R., Fabian A. C., 2005, *MNRAS*, 358, 211
- Ross R. R., Fabian A. C., 2007, *MNRAS*, 381, 1697
- Shakura N. I., Sunyaev R. A., 1973, *A&A*, 500, 33
- Strohmayer T. E., Markwardt C. B., 2002, *ApJ*, 577, 337
- van Paradijs J. et al., 1990, *A&A*, 234, 181
- Verner D. A., Ferland G. J., Korista K. T., Yakovlev D. G., 1996, *ApJ*, 465, 487
- Wijnands R. A. D., van der Klis M., van Paradijs J., Lewin W. H. G., Lamb F. K., Vaughan B., Kuulkers E., 1997, *ApJl*, 479, L141
- Wilms J., Allen A., McCray R., 2000, *ApJ*, 542, 914
- Zdziarski A. A., Johnson W. N., Magdziarz P., 1996, *MNRAS*, 283, 193
- Zhang W., Lapidus I., White N. E., Titarchuk L., 1996, *ApJl*, 469, L17
- Życki P. T., Done C., Smith D. A., 1999, *MNRAS*, 309, 561